Radio-Frequency Orientation of As^{76}†*

F. M. PIPKIN AND J. W. CULVAHOUSE‡
Lyman Laboratory, Harvard University, Cambridge, Massachusetts
(Received October 31, 1957)

Measurements are reported on the successful orientation of 26-hour As^{76} donors in a doped silicon crystal. A general discussion is given of the various methods of dynamic nuclear orientation and how they apply to As^{76}. The use of radio-frequency orientation to determine the sign of the nuclear magnetic moment and the mixture of total angular momenta carried off by the electron-neutrino system is discussed. As^{76} has been oriented by both saturation of forbidden transitions and double resonance methods. The hyperfine splitting of As^{75} in the doped silicon crystal is $+198.42\pm0.04$ Mc/sec; the hyperfine splitting of As^{76} in the same crystal is -93.660 ± 0.06 Mc/sec. The spin of As^{76} has been shown to be 2; its gyromagnetic ratio, -0.4514. The determination of the relative amounts of angular momenta carried off by the $2^-\rightarrow2^+$, 2.41-Mev beta ray gives a result which is consistent with 5 parts $L=0$, 2 parts $L=1$, and 3 parts $L=2$. An unknown systematic error in these last measurements makes it difficult to say precisely what the mixture is. Unsuccessful attempts to produce orientation through the Overhauser and Abragam methods are summarized.

INTRODUCTION

WHEN the work reported in this paper was begun, there were only two proposals for radio-frequency nuclear orientation—one by Kastler[1] and one by Overhauser.[2] An early report by Honig[3] of a long electron relaxation time in arsenic-doped silicon suggested that it might be a good test case for the Overhauser method. It was attractive for two reasons. First, an arsenic-doped silicon crystal could be bombarded with neutrons and part of the stable As^{75} converted into radioactive As^{76}. This would eliminate radiochemical source problems. Second, it displayed resolved hyperfine structure.[4,5] The Overhauser orientation would be produced only at a discrete set of frequencies determined by the hyperfine splitting of the radioactive element. Thus the nuclear orientation could be used to locate the resonance lines and hence determine the magnetic moment of the radioactive element.

Subsequent investigation[6–8] showed that the pattern of relaxation times in the doped silicon crystals was much more complicated than was first assumed. Also three new methods for dynamic nuclear orientation were proposed—one by Feher,[9] one by Jeffries,[10] and one by Abragam.[11,12] Two of these (Feher and Abragam) were suggested by the study of the electron resonances in doped silicon crystals. All of these methods have been tried by us on arsenic-doped silicon; some with and some without success. This paper is a report on the results of these experiments.

In the first section of this paper a brief summary of the various methods of dynamic orientation is given. By some of these methods, changes in nuclear populations which affect only two adjacent nuclear sublevels can be produced. Consequently, the full power of the formal theory of nuclear orientation is not needed. We shall supplement it with an alternate approach which is specialized to the case of As^{76} and which makes it possible to visualize more easily the effects of saturating different electron transitions. In the second section the apparatus is described. The third section comprises a report on the various orientation experiments; the determination of the spin, nuclear magnetic moment, and sign of the nuclear magnetic moment of As^{76} is summarized. A relationship between the contributions of the various angular momenta to the beta decay is derived. Unsuccessful attempts to produce orientation through Overhauser and Abragam methods are summarized. Section four consists of a short discussion of the relationship between the results of this experiment, the nuclear models, and other experiments on beta decay.

THEORY OF THE EXPERIMENT

A. Specification of the Nuclear Orientation

The nuclear decay scheme of 26-hour As^{76}, which has been determined by Kurbatov[13] and co-workers, is shown in Fig. 1. The 2.97-Mev beta ray has a unique first forbidden shape[14]; consequently, the ground state

† This research was supported in part by the joint program of the Office of Naval Research and the U. S. Atomic Energy Commission, the Milton Fund, and the Society of Fellows, Harvard University.

* This research is in part the subject of a thesis submitted by one of the authors (J. W. Culvahouse) to Harvard University in partial fulfillment of the requirements for the degree of Doctor of Philosophy.

‡ National Science Foundation Predoctoral Fellow 1955–1957; now at the Physics Department, University of Oklahoma, Norman, Oklahoma.

[1] A. Kastler, Compt. rend. **233**, 1444 (1951).
[2] A. W. Overhauser, Phys. Rev. **92**, 411 (1953).
[3] A. Honig, Phys. Rev. **96**, 234 (1954).
[4] Fletcher, Yager, Pearson, Holden, Read, and Merritt, Phys. Rev. **94**, 1392 (1954).
[5] Fletcher, Yager, Pearson, and Merritt, Phys. Rev. **95**, 844 (1954).
[6] Feher, Fletcher, and Gere, Phys. Rev. **100**, 1784 (1955).
[7] A. Honig and J. Combrisson, Phys. Rev. **102**, 917 (1956).
[8] A. Abragam and J. Combrisson, Compt. rend. **243**, 576 (1956).
[9] G. Feher, Phys. Rev. **103**, 500 (1956).
[10] C. D. Jeffries, Phys. Rev. **106**, 174 (1957).
[11] A. Abragam, Compt. rend. **242**, 1720 (1956).
[12] A. Abragam and J. Combrisson, Compt. rend. **243**, 650 (1956).
[13] Kurbatov, Murray, and Sakai, Phys. Rev. **98**, 674 (1955).
[14] E. P. Tomlinson and S. L. Ridgway, Phys. Rev. **88**, 170 (1952).

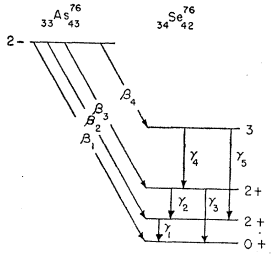

RADIATION	ENERGY	INTENSITY	LOG FT
β_1	2.97	50%	8.8
β_2	2.41	31%	8.2
β_3	1.76	16%	7.9
β_4	0.36	3%	6.1
γ_1	0.55	100	EQ
γ_2	0.64	20	MD+EQ
γ_3	1.20	21	EQ
γ_4	1.40	2	—
γ_5	2.05	1	—

FIG. 1. Nuclear energy level diagram for As^{76}.

of As^{76} is assumed to have a spin of 2 and negative parity. The radiation β_2 is a first forbidden transition with an allowed spectrum shape.[15] It also displays beta-gamma angular correlation[16]; it is assumed that the emitted electron-neutrino system is a mixture of total angular momentum $L=0$, $L=1$, and $L=2$ components for this 2^- to 2^+ transition. The spins and parities of the levels of Se^{76} have been assigned from a study of the gamma-gamma and the beta-gamma angular correlations.[17–19] The radiations γ_1 and γ_3 are pure electric quadrupole; the radiation γ_2 is a mixture of $(98\pm1)\%$ electric quadrupole and $(2\pm1)\%$ magnetic dipole radiation.[20] The lifetime of the 550-kev state of Se^{76} has been measured by Coulomb excitation[21] and coincident methods.[22] It is approximately 2×10^{-11} second.

In the orientation experiments the gamma rays are observed. The principal contribution to the counting rate is from γ_1. To calculate the orientation parameters, two schemes will be used. The first method employs the general theory of nuclear orientation due to De Groot, Cox, and Tolhoek[23]; it is useful for calculating the change in orientation parameters due to the angular momentum carried off by the beta ray. The second method requires only knowledge of the angular distributions for electric quadrupole radiation; it is useful as a means of quickly visualizing the effect of applying different radio-frequency fields. Let j_0, j_i, and j_f designate the spins of As^{76}, the gamma-emitting state of Se^{76} and the final state to which the gamma ray decays, respectively. If $j_f=j_i-2$, the angular distribution[24] of the electric quadrupole gamma ray will be given by

$$N(\theta)=2\{1-(15/7)N_2f_2P_2(\cos\theta)-5N_4f_4P_4(\cos\theta)\}, \quad (1)$$

where

$$N_2=\frac{j_i}{2j_i-1}, \quad N_4=\frac{j_i^3}{(j_i-1)(2j_i-1)(2j_i-3)}, \quad (2)$$

$$f_2(j_i)=\frac{1}{j_i^2}[\sum_{m_i} m_i^2a_{m_i}-\tfrac{1}{3}j_i(j_i+1)], \quad (3)$$

$$f_4(j_i)=\frac{1}{j_i^4}[\sum_{m_i} m_i^4a_{m_i}-(1/7)(6j_i^2+6j_i-5)\sum_{m_i} a_{m_i}m_i^2 +(3/35)(j_i)(j_i-1)(j_i+1)(j_i+2)], \quad (4)$$

and the spherical harmonics are given by

$$P_2=\tfrac{3}{2}(\cos^2\theta-\tfrac{1}{3}), \quad (5)$$

$$P_4=(35/8)[\cos^4\theta-(6/7)\cos^2\theta+(3/35)]. \quad (6)$$

The a_{m_i} are the populations of the nuclear sublevels normalized so that

$$\sum_{m_i} a_{m_i}=1.$$

The f_2 and f_4 parameters for the intermediate gamma emitting state of spin j_i are related to the f_2 and f_4 parameters of the parent As^{76} by the equation[23]

$$f_k(j_i)=\sum_L \alpha_L\frac{w_k(j_i)}{w_k(j_0)}(2j_0+1)W(j_iLkj_0;\, j_0j_i)f_k(j_0), \quad (7)$$

where

$$\frac{w_k(j_i)}{w_k(j_0)}=\left[\frac{(2j_i+k+1)\,!(2j_0-k)\,!}{(2j_i-k)\,!(2j_0+k+1)\,!}\right]^{\frac{1}{2}}\left(\frac{j_0}{j_i}\right)^k, \quad (8)$$

and

$$\alpha_L'=\int_1^{W_0} S_L(W)F(W,Z)dW. \quad (9)$$

$W(j_iLkj_0;\, j_0j_i)$ is a Racah coefficient; $F(W,Z)$ is the Fermi function for beta decay; and S_L is the shape factor[24] for the component of the beta decay in which the electron-neutrino system is emitted into a state of total angular momentum L. For a first-forbidden 2^- to 2^+ transition as in As^{76}, the summation is over L values of 0, 1, and 2. It is convenient to introduce a new set of parameters,

$$\alpha_L=\alpha_L'/\sum\alpha_L',$$

such that

$$\sum\alpha_L=1. \quad (10)$$

In a radio-frequency alignment experiment, there is generally a large electromagnet around the sample; consequently, it is difficult to move the counter. The orientation can, however, be produced and destroyed in a short time. Thus the meaningful signal is the change in counting rate at a given angle when the orientation is produced. These fractional changes in counting rate will be called the signals and designated by the symbols $S(\pi)$ and $S(\sigma)$. The spectroscopic σ and π notation is used to designate the directions of observation per-

[15] Pohm, Waddell, and Jensen, Phys. Rev. **101**, 1315 (1956).
[16] H. Rose, Phil. Mag. **44**, 739 (1953).
[17] Hamilton, Lemonick, and Pipkin, Phys. Rev. **92**, 1191 (1953).
[18] J. J. Kraushaar and M. Goldhaber, Phys. Rev. **89**, 1081 (1953).
[19] F. R. Metzger and W. B. Todd, J. Franklin Inst. **256**, 257 (1953).
[20] T. Lindquist and I. Morklund, Nuclear Phys. **4**, 189 (1957).
[21] G. M. Temmer and N. P. Heydenburg, Phys. Rev. **104**, 967 (1956).
[22] C. F. Coleman, Phil. Mag. **46**, 1135 (1955).
[23] S. R. De Groot and H. A. Tolhoek in *Beta- and Gamma-Ray Spectroscopy*, edited by K. Siegbahn (North Holland Publishing Company, Amsterdam, 1955), Chap. 19, Part III, p. 613.
[24] E. Konopinski in *Beta- and Gamma-Ray Spectroscopy*, edited by K. Siegbahn (North Holland Publishing Company, Amsterdam, 1955), Chap. 10, p. 292.

pendicular to and parallel to the magnetic field, respectively. In terms of the f_k parameters, the signals are

$$S(\sigma)=(5/7)f_2-5f_4, \tag{11}$$

$$S(\pi)=-(10/7)f_2-(40/3)f_4. \tag{12}$$

For discussion of the various methods for orientation, it will be assumed that the beta ray carries away no angular momentum. In this case and for a $2^-\rightarrow 2^+\rightarrow 0$ transition as in As^{76}, an alternative method can be used to calculate the signals. Since the beta ray carries away no angular momentum, the populations of the nuclear sublevels of As^{76} are the same as those of the excited state of Se^{76}. The situation is no different from the case where a gamma-ray-emitting nucleus is being aligned. The angular distributions for a quadrupole gamma ray are shown in Fig. 2. From these diagrams it is clear that

$$S(\sigma)=\tfrac{1}{4}(1-5a_0), \tag{13}$$

$$S(\pi)=\tfrac{1}{2}(5a_1+5a_{-1}-2). \tag{14}$$

The population of the levels a_1 and a_{-1} entirely determines the radiation emitted in the direction of the magnetic field; the change in emission perpendicular to the direction of the magnetic field is due to changes in a_0.

B. Energy Levels of the Donor Atom in a Magnetic Field

The electronic ground state for a group V donor atom in a silicon crystal is a $^2S_{\frac{1}{2}}$ state. In a magnetic field, the interaction between the nucleus and the electronic spin is described by the Hamiltonian

$$H=-g_J\mu_0(\mathbf{J}\cdot\mathbf{H})-g_I\mu_n(\mathbf{I}\cdot\mathbf{H})+A(\mathbf{I}\cdot\mathbf{J}), \tag{15}$$

where g_J is the electron gyromagnetic ratio, g_I the nuclear gyromagnetic ratio, μ_0 the Bohr magneton, μ_n the nuclear magneton, A the hyperfine interaction constant, and H the magnetic field. The gyromagnetic ratio of the electron is taken to be negative and A is positive for a positive nuclear moment. The energy levels in a large ($\mu_0H\gg A$) magnetic field can be expressed in terms of the quantum numbers of the uncoupled nucleus and electron. Correct to the second order in the hyperfine interaction, the energy levels for a donor atom with a $^2S_{\frac{1}{2}}$ ground state are given by

$$E_{m_J,m_I}=-g_J\mu_0Hm_J-g_I\mu_nHm_I+Am_Im_J+(A^2/4\mu_0H)m_J(I-2m_Jm_I)\times(I+2m_Jm_I+1). \tag{16}$$

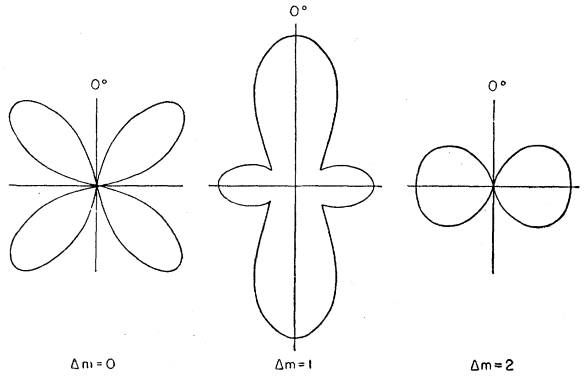

FIG. 2. Angular distributions for quadrupole radiation. All the diagrams are drawn to the same scale so that relative emission probabilities can be determined by comparison of corresponding radii.

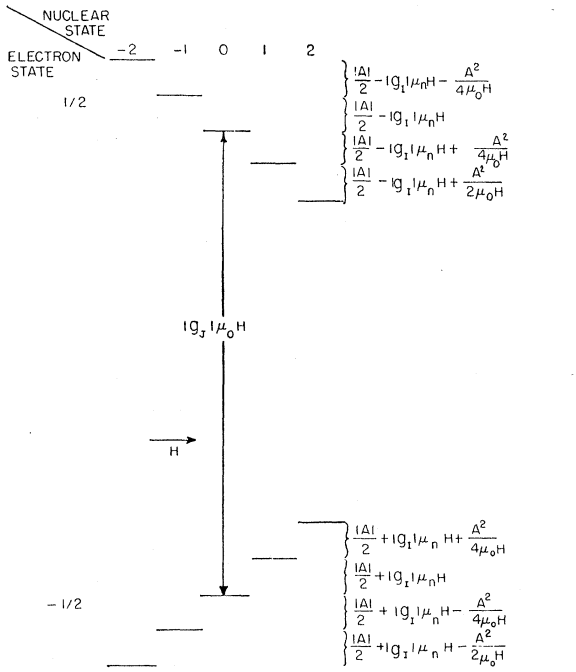

FIG. 3. Energy levels for donor atom with nuclear spin 2 and a negative nuclear magnetic moment in a large magnetic field ($2\mu_0H\gg A$). The arrow with the H indicates the order in which the lines are displayed as a function of magnetic field with a fixed oscillator frequency.

Figure 3 shows the energy levels for nuclear spin 2 and a negative nuclear magnetic moment; Fig. 4 shows the energy levels for nuclear spin 2 and a positive nuclear magnetic moment. The small numbers beside the levels in Fig. 4 represent the relative populations for a field of 8500 gauss and a temperature of 1.25°K. In subsequent discussions the various levels will be denoted by the number pairs (m_J,m_I).

To the first order in the hyperfine coupling, the wave functions of the levels are

$$\varphi(m_J,m_I)=\psi(\tfrac{1}{2},m_J)\chi(I,m_I)-(m_JA/g_J\mu_0H)\times[(I-2m_Im_J)(I+2m_Jm_I+1)]^{\frac{1}{2}}\times\psi(\tfrac{1}{2},-m_J)\chi(I,m_I+2m_J). \tag{17}$$

Each level with a given total (m_I+m_J) value contains a mixture of the level $(-m_J,m_I+2m_J)$. Consequently, if a radio-frequency field which has a component along

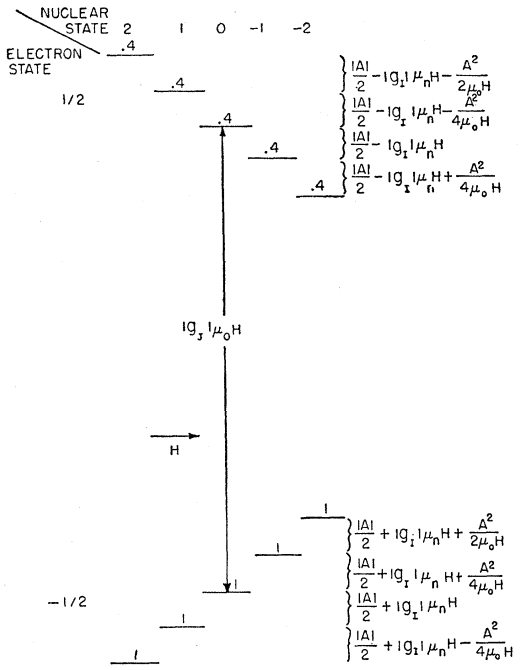

FIG. 4. Energy levels for a donor atom with nuclear spin 2 and a positive nuclear magnetic moment in a large magnetic field ($2\mu_0 H \gg A$). The arrow with the H indicates the order in which the lines are displayed as a function of magnetic field with a fixed oscillator frequency.

the axis of quantization is applied to the atom, transitions can be induced between the level (m_J, m_I) and the level $(-m_J, m_I+2m_J)$ via the weak coupling due to the hyperfine interaction.

C. Methods of Dynamic Nuclear Orientation

The first method of orientation which will be discussed was suggested by Jeffries.[10] Although it was the last to be suggested, it is the simplest to discuss. This method utilizes the saturation of the forbidden $\Delta(m_J+m_I)=0$ transitions. Consider the saturation of the transition $(-\frac{1}{2},+1)\rightarrow(\frac{1}{2},0)$, which is shown schematically in Fig. 5. In this figure and in the rest of this paper the abbreviation

$$\alpha=\exp(-2\mu_0 H/kT) \tag{18}$$

has been used. For 1.25°K and 8500 gauss, $\alpha=0.4$. The first effect of the radio-frequency field is to equalize the population of the $(-\frac{1}{2},1)$ and the $(\frac{1}{2},0)$ levels as shown in Fig. 5(b). If the nuclear relaxation time is assumed to be long compared with the electron relaxation time, the orientation will increase until the final equilibrium state shown in Fig. 5(c) is reached. If Eqs. (13) and (14) are used to calculate the signals for the transition, the expressions

$$S(\sigma)=-\tfrac{1}{4}\tanh(\mu_0 H/kT), \tag{19}$$

$$S(\pi)=-\tfrac{1}{2}\tanh(\mu_0 H/kT) \tag{20}$$

TABLE I. Signals expected for saturation of the forbidden transitions. The β decay is assumed to be pure $L=0$.

Transition	Signals $S(\sigma)$	$S(\pi)$
$(-\frac{1}{2},2)\rightarrow(\frac{1}{2},1)$	0.00	+0.22
$(-\frac{1}{2},1)\rightarrow(\frac{1}{2},0)$	−0.11	−0.22
$(-\frac{1}{2},0)\rightarrow(\frac{1}{2},-1)$	+0.11	+0.22
$(-\frac{1}{2},1)\rightarrow(\frac{1}{2},-2)$	0.00	−0.22

are obtained. The saturation of the $(-\frac{1}{2},1)\rightarrow(\frac{1}{2},0)$ transition increases the population of the $m=0$ level and decreases the population of the $m=1$ level; consequently, the counting rate is decreased in both the σ and π positions. Comparison of Fig. 5 with Figs. 3 and 4 shows that for a negative nuclear moment the transition $(-\frac{1}{2},1)\rightarrow(\frac{1}{2},0)$ will be the third forbidden transition starting at zero magnetic field with a fixed oscillator frequency; for a positive nuclear moment it will be the second forbidden transition. The signals depend only upon the transition saturated; the order of the transition in magnetic field depends upon the sign of the nuclear magnetic moment. In Table I are summarized the signals which should be obtained by saturating the various forbidden transitions at 1.25°K and 8500 gauss. This simple picture will be true only if the nuclear relaxation times are much longer than the time required to saturate the forbidden transitions and observe the orientation. If the nuclear relaxation time is comparable with the time required to saturate the forbidden transition, the equilibrium configuration will be more

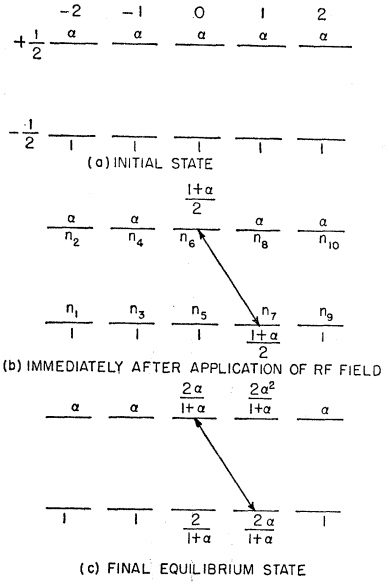

FIG. 5. Schematic representation of the saturation of the forbidden transition $(-\frac{1}{2},1)\rightarrow(\frac{1}{2},0)$. The numbers besides the levels represent the relative populations. The symbol α has been introduced for $\exp(-2\mu_0 H/kT)$; for 8500 gauss and 1.25°K, $\alpha=0.4$. This transition increases the population of the nuclear $m=0$ level at the expense of the $m=1$ level. The nuclear relaxation time has been assumed to be much longer than the electron-only relaxation time.

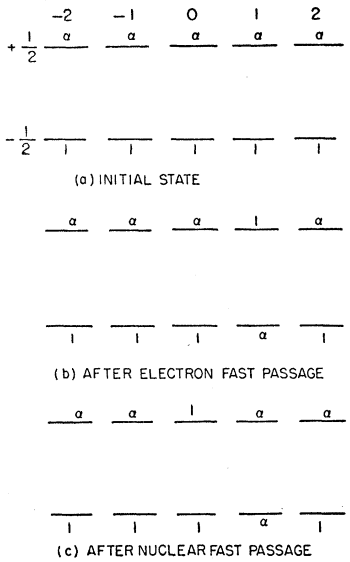

FIG. 6. Schematic representation of the production of orientation by the double fast-passage method. α equals $\exp(-2\mu_0 H/kT)$. The electron fast passage inverts the levels $(\frac{1}{2},1)$ and $(-\frac{1}{2},1)$; the nuclear fast passage inverts the levels $(\frac{1}{2},0)$ and $(\frac{1}{2},+1)$.

complicated and usually the signals obtained smaller. Since the nuclear relaxation time in As^{76} is long,[25] the more complicated case will not be considered.

The second method which will be discussed was suggested by Feher[9]; it uses two radio-frequency fields to produce the orientation. The most efficient way to rearrange the nuclear populations in this fashion is to use the technique of adiabatic fast passage to invert the populations of the levels. Consider the sequence shown in Fig. 6. First the level pair $(-\frac{1}{2},1)$, $(\frac{1}{2},1)$ is inverted with a microwave radio-frequency field, then the pair $(\frac{1}{2},1)$, $(\frac{1}{2},0)$ is inverted with a low-frequency field. This sequence produces an orientation of the same magnitude as was obtained by saturation of the forbidden transition $(-\frac{1}{2},1)\rightarrow(\frac{1}{2},0)$. This method has the advantage that a given sign of alignment can be produced independent of the sign of the nuclear magnetic moment. This will be discussed more fully in the section on the determination of the sign of the nuclear magnetic moment. The double fast-passage method also makes it possible to do several successive operations and increase the population of a given nuclear sublevel at the expense of several other sublevels. The fact that it requires the use of two radio-frequency fields makes it difficult to use as a search method when the hyperfine splitting is unknown.

The third method, which will be discussed, was suggested by Kastler[1]; this method was historically the first to be suggested. It replaces the two fast-passage operations by two saturating radio-frequency fields. This makes the method applicable to more substances, but decreases the orientation produced.

[25] J. W. Culvahouse and F. M. Pipkin, Phys. Rev. **109**, 319 (1958).

The fourth method, which was proposed by Abragam,[11] utilizes the change in the structure of the electron-nucleus wave function when the magnetic field is changed adiabatically from a high value such that $\mu_0 H \gg A$ to a low value such that $\mu_0 H \ll A$. The energy levels of a donor atom with nuclear spin 2 and a negative nuclear magnetic moment as a function of magnetic field are shown in Fig. 7. In Table II the wave functions of the donor atom at high and low magnetic field are listed. From these wave functions and the populations of the levels in high magnetic field, the nuclear populations and hence the orientation signals can be calculated. The results of these calculations are summarized in Table III. This table shows that upon reduction of the magnetic field from an initial value of 11 000 gauss at 1.25°K to a value of 10 gauss a considerable nuclear polarization would be produced. In low magnetic field, however, the energy separations in the $F=I+\frac{1}{2}$ and the $F=I-\frac{1}{2}$ complexes become equal. Consequently, spin-spin interactions can set in between the adjacent donors; this will establish a Boltzmann distribution over the levels of the two groups. The results of such an exchange upon the orientation are shown in Table III. If the sample is now returned to high field, a simple calculation shows that there will again be a net orientation; this is also listed in Table III. The process of going from high to low exchanging and then going back to high field can be repeated a number of times with a gain in orientation each time. The successful attainment of orientation by this method is complicated by the possibly short spin-lattice relaxation time in low magnetic fields and the transitions produced by exchange interactions which may occur due to accidental energy level equalities produced during the transit from high to low to high magnetic field.

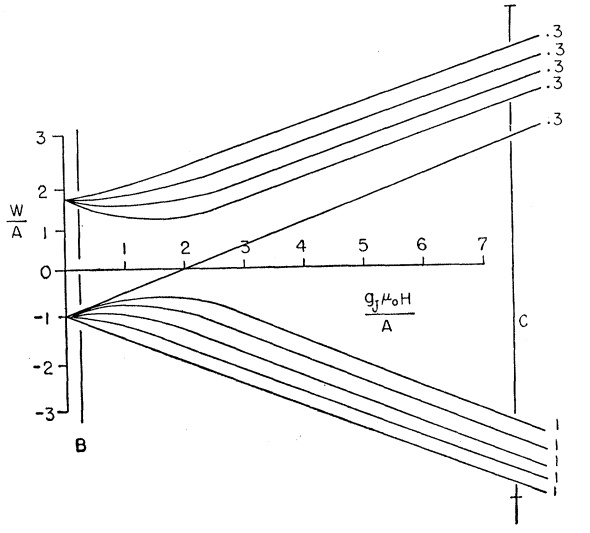

FIG. 7. Energy levels as a function of magnetic field of donor atom with spin 2 and a negative nuclear magnetic moment. The small numbers beside the levels represent the relative population for 11 000 gauss and 1.22°K.

TABLE II. Wave functions at high ($\mu_0 H \ll A$) and low ($\mu_0 H \ll A$) magnetic field for an electron coupled to a nucleus of spin 2 having a negative nuclear magnetic moment. The small residual impurity in the high-field wave function has been ignored.

High-field state	High-field wave function	Low-field wave function
$(\frac{1}{2},-2)$	$\varphi(\frac{1}{2},\frac{1}{2})\psi(2,-2)$	$-(\frac{4}{5})^{\frac{1}{2}}\varphi(\frac{1}{2},\frac{1}{2})\psi(2,-2)+(\frac{1}{5})^{\frac{1}{2}}\varphi(\frac{1}{2},-\frac{1}{2})\psi(2,-1)$
$(\frac{1}{2},-1)$	$\varphi(\frac{1}{2},\frac{1}{2})\psi(2,-1)$	$-(\frac{3}{5})^{\frac{1}{2}}\varphi(\frac{1}{2},\frac{1}{2})\psi(2,-1)+(\frac{2}{5})^{\frac{1}{2}}\varphi(\frac{1}{2},-\frac{1}{2})\psi(2,0)$
$(\frac{1}{2},0)$	$\varphi(\frac{1}{2},\frac{1}{2})\psi(2,0)$	$-(\frac{2}{5})^{\frac{1}{2}}\varphi(\frac{1}{2},\frac{1}{2})\psi(2,0)+(\frac{3}{5})^{\frac{1}{2}}\varphi(\frac{1}{2},-\frac{1}{2})\psi(2,+1)$
$(\frac{1}{2},1)$	$\varphi(\frac{1}{2},\frac{1}{2})\psi(2,1)$	$-(\frac{1}{5})^{\frac{1}{2}}\varphi(\frac{1}{2},\frac{1}{2})\psi(2,+1)+(\frac{4}{5})^{\frac{1}{2}}\varphi(\frac{1}{2},-\frac{1}{2})\psi(2,+2)$
$(\frac{1}{2},2)$	$\varphi(\frac{1}{2},\frac{1}{2})\psi(2,2)$	$\varphi(\frac{1}{2},\frac{1}{2})\psi(2,2)$
$(-\frac{1}{2},+2)$	$\varphi(\frac{1}{2},-\frac{1}{2})\psi(2,2)$	$(\frac{4}{5})^{\frac{1}{2}}\varphi(\frac{1}{2},\frac{1}{2})\psi(2,1)+(\frac{1}{5})^{\frac{1}{2}}\varphi(\frac{1}{2},-\frac{1}{2})\psi(2,2)$
$(-\frac{1}{2},1)$	$\varphi(\frac{1}{2},-\frac{1}{2})\psi(2,+1)$	$(\frac{3}{5})^{\frac{1}{2}}\varphi(\frac{1}{2},\frac{1}{2})\psi(2,0)+(\frac{2}{5})^{\frac{1}{2}}\varphi(\frac{1}{2},-\frac{1}{2})\psi(2,1)$
$(-\frac{1}{2},0)$	$\varphi(\frac{1}{2},-\frac{1}{2})\psi(2,0)$	$(\frac{2}{5})^{\frac{1}{2}}\varphi(\frac{1}{2},\frac{1}{2})\psi(2,-1)+(\frac{3}{5})^{\frac{1}{2}}\varphi(\frac{1}{2},-\frac{1}{2})\psi(2,0)$
$(-\frac{1}{2},-1)$	$\varphi(\frac{1}{2},-\frac{1}{2})\psi(2,-1)$	$(\frac{1}{5})^{\frac{1}{2}}\varphi(\frac{1}{2},\frac{1}{2})\psi(2,-2)+(\frac{4}{5})^{\frac{1}{2}}\varphi(\frac{1}{2},-\frac{1}{2})\psi(2,-1)$
$(-\frac{1}{2},-2)$	$\varphi(\frac{1}{2},-\frac{1}{2})\psi(2,-2)$	$+\varphi(\frac{1}{2},-\frac{1}{2})\psi(2,-2)$

The fifth method is a generalization of a proposal originally suggested by Overhauser.[2] It relies upon the special nature of certain nuclear relaxation processes to produce the orientation. The general relaxation scheme for a donor atom with nuclear spin 2 is shown in Fig. 8. T_s is the relaxation time for processes in which only the electron spin changes state; T_x is the relaxation time for processes in which the nucleus and electron flip simultaneously so that $\Delta(m_I+m_J)=0$. This second process occurs only between the levels coupled by the hyperfine interaction. If a microwave magnetic field is applied so as to saturate the $(-\frac{1}{2},0)\rightarrow(\frac{1}{2},0)$ electron transition the orientation will develop as shown in Fig. 9. In Table IV are summarized the expected orientations produced by saturation of the various single electron transitions and by simultaneous saturation of all of them. This latter case corresponds to the original Overhauser proposal.

TABLE III. The nuclear populations and expected alignment signals for the various Abragam methods of orientation. A represents the initial high-field configuration, B the configuration after going to low field, C the configuration after exchange sets in at low field, and D the configuration after going back up to high field. A pure ($L=0$) β ray has been assumed. The initial conditions are 11 000 gauss and 1.22°K.

Situation	Nuclear populations a_{-2}	a_{-1}	a_0	a_1	a_2	Signals $S(\pi)$	$S(\sigma)$
A	0.200	0.200	0.200	0.200	0.200	0.000	0.000
B	0.222	0.222	0.222	0.222	0.114	0.110	−0.028
C	0.246	0.221	0.197	0.176	0.158	−0.008	0.004
D	0.226	0.205	0.188	0.172	0.216	−0.058	0.016

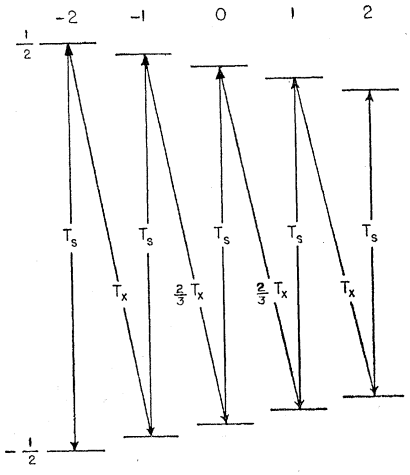

FIG. 8. Energy level diagram for donor atom with nuclear spin 2 showing the two electron relaxation times. T_S is the relaxation time for spin flips of the electron alone; T_X is the relaxation time for processes in which the electron and the nucleus flip simultaneously so that $\Delta(m_I+m_J)=0$.

D. Influence of the β Decay

If Eqs. (7) to (9) are evaluated for the general $2^-\rightarrow 2^+$ β transition of As^{76}, Eq. (1) becomes

$$N(\theta)=2\left[1-\frac{10}{7}\left(1-\frac{\alpha_1}{2}-\frac{17\alpha_2}{14}\right)f_2P_2 - \frac{40}{3}\left(1-\frac{5\alpha_1}{3}-\frac{5\alpha_2}{7}\right)f_4P_4\right]. \quad (21)$$

The normalization condition, Eq. (10), has been used to eliminate α_0. Equation (21) can be used to find the signals expected for an arbitrary mixture of angular momentum carried off by the electron-neutrino system. If the nuclear relaxation time is long compared with the time of formation of the orientation, simple expressions can be derived for the signals. For both the case of orientation produced by saturation of a forbidden transition and the double-resonance methods, the final nuclear populations can be expressed in the form

$$\begin{aligned} 5a_{-2}&=1,\\ 5a_{-1}&=1+\eta\tanh(\mu_0H/kT),\\ 5a_0&=1-\eta\tanh(\mu_0H/kT),\\ 5a_{+1}&=1,\\ 5a_{+2}&=1. \end{aligned} \quad (22)$$

This particular example is for processes which change the populations of the a_{-1} and the a_0 nuclear sublevels. For the saturation of the forbidden transitions,

$$0\leq\eta\leq 1.$$

In the case of orientation produced by using two radio-frequency fields,

$$-1\leq\eta\leq 1.$$

TABLE IV. Nuclear populations and alignment signals expected for Overhauser effect. Situation A represents the saturation of all five transitions simultaneously. A pure ($L=0$) β ray has been assumed. Calculations were made for $T=1.25°$K and $H=8500$ gauss.

Transition being saturated	Nuclear populations					Signals	
	a_{-2}	a_{-1}	a_0	a_1	a_2	$S(\pi)$	$S(\sigma)$
$(\frac{1}{2},-2)\rightarrow(-\frac{1}{2},-2)$	0.125	0.218	0.218	0.218	0.218	+0.090	−0.023
$(\frac{1}{2},-1)\rightarrow(-\frac{1}{2},-1)$	0.100	0.144	0.252	0.252	0.252	−0.010	−0.065
$(\frac{1}{2},0)\rightarrow(-\frac{1}{2},0)$	0.119	0.119	0.170	0.297	0.297	+0.040	+0.038
$(\frac{1}{2},+1)\rightarrow(-\frac{1}{2},+1)$	0.144	0.144	0.144	0.206	0.361	−0.125	+0.070
$(\frac{1}{2},+2)\rightarrow(-\frac{1}{2},+2)$	0.185	0.185	0.185	0.185	0.264	−0.075	+0.019
A	0.016	0.039	0.097	0.242	0.606	−0.298	+0.129

The parameter η will be called the efficiency of orientation; it measures how closely the thermodynamic maximum is approached. The f_2 and f_4 parameters can be readily computed for nuclear populations of the form of Eqs. (22). For saturation of the $(-\frac{1}{2},2)\rightarrow(\frac{1}{2},1)$ transition,

$$f_2=-(3\eta/20)\tanh(\mu_0H/kT), \tag{23}$$

$$f_4=-(3\eta/140)\tanh(\mu_0H/kT). \tag{24}$$

For saturation of the $(-\frac{1}{2},1)\rightarrow(\frac{1}{2},0)$ transition,

$$f_2=-(\eta/20)\tanh(\mu_0H/kT), \tag{25}$$

$$f_4=(3\eta/70)\tanh(\mu_0H/kT). \tag{26}$$

Equation (21) can now be used to write the signals for an arbitrary beta-decay mixture in terms of the efficiency. For the transition $(-\frac{1}{2},2)\rightarrow(\frac{1}{2},1)$ the expressions

$$S_O(\pi)=\frac{\eta}{2}\left(1-\frac{7\alpha_1}{6}-\frac{13\alpha_2}{14}\right)\tanh\left(\frac{\mu_0H}{kT}\right), \tag{27}$$

$$S_O(\sigma)=-\frac{\eta}{4}\left(\frac{\alpha_1}{2}-\frac{3\alpha_2}{14}\right)\tanh\left(\frac{\mu_0H}{kT}\right) \tag{28}$$

are obtained. The subscript O has been introduced to signify that this transition is one of the outer pair of forbidden transitions. For the transition $(-\frac{1}{2},1)\rightarrow(\frac{1}{2},0)$ the signals are given by

$$S_I(\pi)=-\frac{\eta}{2}\left(1-\frac{11\alpha_1}{6}-\frac{9\alpha_2}{14}\right)\tanh\left(\frac{\mu_0H}{kT}\right), \tag{29}$$

$$S_I(\sigma)=-\frac{\eta}{4}\left(1-\frac{3\alpha_1}{2}-\frac{11\alpha_2}{14}\right)\tanh\left(\frac{\mu_0H}{kT}\right). \tag{30}$$

The subscript I designates that this is one of the inner pair of forbidden transitions. The expressions for the other two transitions can be obtained by changing the sign of η; the whole pattern for saturation of the forbidden transitions is always antisymmetric about its center. In order to demonstrate the sensitivity of the results to the character of the beta decay, in Table V are summarized the expected signals for various combinations of angular momentum carried off by the electron-neutrino system.

From the measured signals for the σ and π positions and the same orientation configuration, the two ratios

$$r_I=S_I(\sigma)/S_I(\pi), \tag{31}$$

$$r_O=S_O(\sigma)/S_O(\pi), \tag{32}$$

can be calculated. These two ratios are independent of efficiency but not independent of each other. The following relationship exists between them

$$3+4r_O-6r_I-16r_Or_I=0. \tag{33}$$

TABLE V. Calculated value of signals expected for various combinations of total angular momentum carried off by the electron-neutrino system. Calculations were made for $T=1.25°$K and $H=8500$ gauss. S_I denotes the $(-\frac{1}{2},1)\rightarrow(\frac{1}{2},0)$ transition and S_O denotes the $(-\frac{1}{2},2)\rightarrow(\frac{1}{2},1)$ transition.

Beta-decay mixture			Signals			
α_0	α_1	α_2	$S_I(\pi)$	$S_I(\sigma)$	$S_O(\pi)$	$S_O(\sigma)$
1	0	0	−0.215	−0.108	0.215	0.000
0	1	0	+0.179	+0.054	−0.036	−0.054
0	0	1	−0.078	−0.023	0.014	+0.023
0.33	0.33	0.34	−0.038	−0.026	0.065	−0.010
0.40	0.45	0.15	−0.017	−0.022	0.072	−0.021
0.39	0.27	0.34	−0.062	−0.035	0.079	−0.007

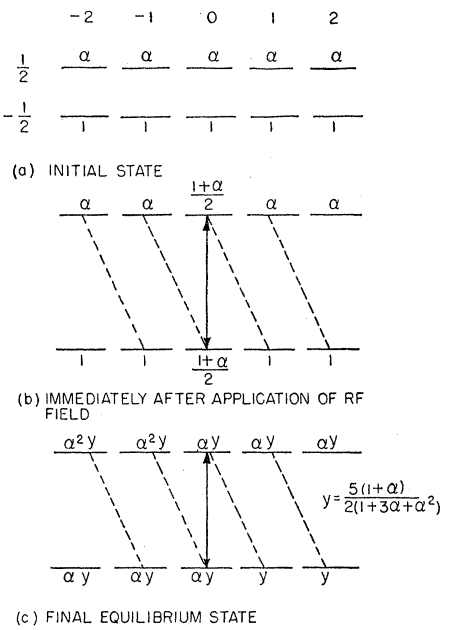

FIG. 9. Schematic representation of the formation of orientation by saturation of the transition $(\frac{1}{2},0)\rightarrow(-\frac{1}{2},0)$. The dotted lines represent the relaxation paths which produce the orientation.

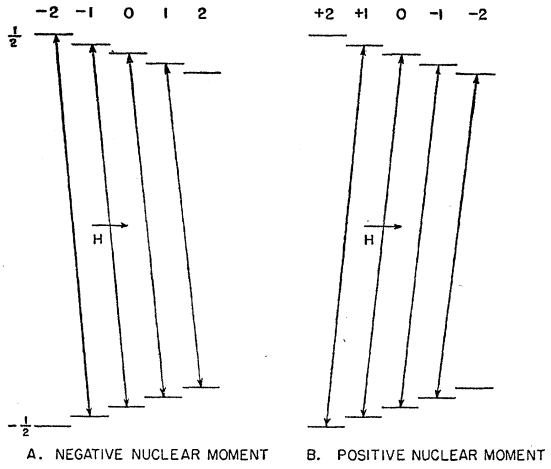

FIG. 10. Energy level diagrams for spin 2 donors showing the difference produced in the forbidden transitions when the sign of the moment is changed. The arrow with an H indicates the order in which the lines are displayed as the field is increased with a fixed oscillator frequency.

Thus from the two equations, (31) and (32), one linear relationship between α_1 and α_2 can be obtained.

E. Determination of the Sign of the Nuclear Magnetic Moment

One advantage of using the radio-frequency orientation method to measure nuclear magnetic moments is that the sign of the moment enters in a natural fashion. There are three ways in which the sign can be determined. The first method utilizes a double resonance experiment to interpret the results of the saturation of a forbidden transition.

In Fig. 10 are shown the level schemes and the forbidden transitions for both positive and negative nuclear magnetic moments. Without knowledge of the sign of the nuclear magnetic moment, it cannot be determined whether the highest forbidden transition in magnetic field is $(-\frac{1}{2},-1)\rightarrow(\frac{1}{2},-2)$ or $(-\frac{1}{2},2)\rightarrow(\frac{1}{2},1)$. In the first case saturation of the high-field forbidden transition increases the population of the $m_I=-2$ nuclear sublevel at the expense of the $m_I=-1$ sublevel; in the second case, the population of the $m_I=1$ level is increased at the expense of the $m_I=2$ level. If alignment is being observed, the effects are of the same magnitude but of opposite sign. An examination of the energy levels in Figs. 3 and 4 shows that a double resonance experiment can always be performed which produces a known sign of alignment. This can be achieved by inverting the highest electron transition in magnetic field and then inverting the highest frequency nuclear transition. For a positive nuclear magnetic moment, this sequence increases the population of the $m_I=-2$ level and decreases the population of the $m_I=-1$ level; for a negative nuclear magnetic moment, this sequence increases the population of the $m_I=2$ level and decreases the population of the $m_I=1$ level. In each case the alignment produced is the same. This technique can be used to determine the sign of the anisotropy produced when there are more nuclei in the $m=2$ ($m=-2$) level than the $m=1$ ($m=-1$) level. Comparison of this sign with the sign of the effect obtained by saturation of the high-field forbidden transition immediately yields the sign of the nuclear magnetic moment.

The second method for determining the sign of the nuclear magnetic moment utilizes the correlation between the sign of the signals and the relative position of the forbidden lines as a function of magnetic field. Figures 11 and 12 show the calculated signal patterns for various angular momenta carried off by the electron-neutrino system and the two signs of the nuclear magnetic moment. If the relative probability for emission of the electron-neutrino system with a given angular momentum can be determined, then the sign can be determined in this fashion. The only real ambiguity occurs when there is a mixture of $L=1$ and $L=2$ alone. The $L=2$ patterns are the same as the $L=1$ patterns but with opposite sign and reduced magnitude. The same type of antisymmetric patterns exist for the Overhauser orientation.

The third method is by comparison of the center of gravity of the forbidden transitions and that of the electron resonance lines of the stable isotope. For the stable isotope the center of gravity of the electron lines is at

$$H=h\nu/(|g_J|\mu_0), \tag{34}$$

where ν is the oscillator frequency. For the forbidden

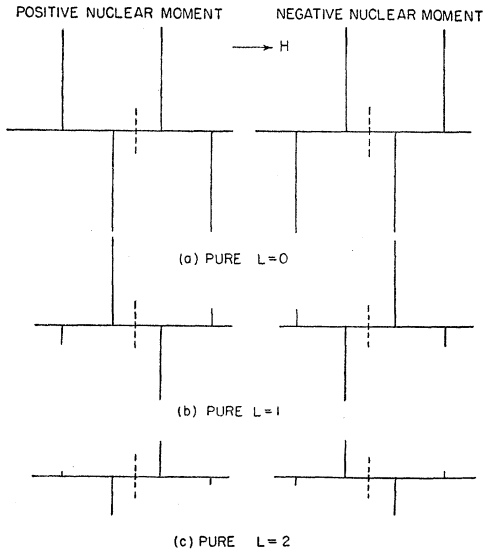

FIG. 11. Signals expected in the π position as a function of magnetic field for various angular momenta carried off by the electron-neutrino system. The arrow with an H indicates the order in which the lines are displayed as a function of magnetic field for a fixed oscillator frequency. The dotted line indicates the center of the hyperfine structure. All signals are drawn to scale and the same scale is used in Fig. 12.

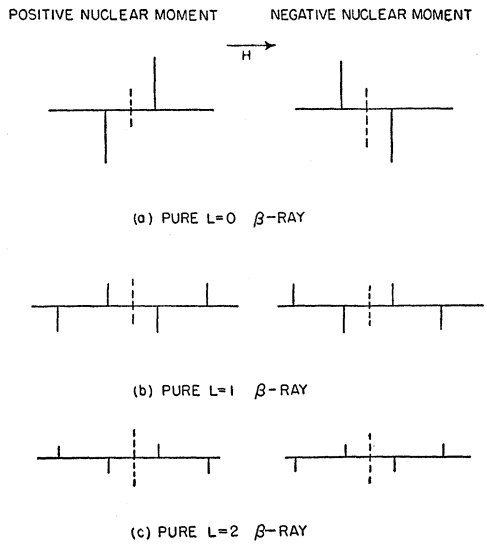

FIG. 12. Signals expected in the σ position as a function of magnetic field for various angular momenta carried off by the electron-neutrino system. The arrow with an H indicates the order in which the lines are displayed as a function of magnetic field for a fixed oscillator frequency. The dotted line indicates the center of the hyperfine structure. All signals are drawn to the same scale as in Fig. 11.

transitions, the center of gravity is at

$$H=h\nu/(|g_J|\mu_0+g_I\mu_n). \quad (35)$$

Thus the direction of the shift depends upon the sign of the nuclear magnetic moment.

EXPERIMENTAL APPARATUS

Experiments on radio-frequency orientation require the general apparatus of paramagnetic resonance spectroscopy plus nuclear counting equipment for observation of the changes in counting rate. The paramagnetic resonance spectrometer can be quite simple; however, since the anticipated changes in counting rate are small, the counters must be very stable.

For this experiment an electromagnet with a 3-in. gap and 9-in. diameter pole pieces was used. This magnet was originally designed by Professor Bainbridge. The magnet is provided with Rose[26] shims and with the present generator will produce a field of 11 000 gauss. A simple galvanometer feedback system regulates the magnet current by controlling the generator field excitation. Various motor-driven potentiometers in the feedback loop provides a variety of magnetic field sweep patterns. The magnetic field is monitored continuously with a proton resonance detector using the simple Hopkins circuit.[27]

The paramagnetic resonance spectrometer uses a magic-T bridge to observe the changes in the reflection coefficient of the cavity which contains the sample. A block diagram is shown in Fig. 13. The spectrometer operates at 24 000 Mc/sec; this frequency was chosen as the highest frequency for which oscillators with adequate power (10 milliwatts in the cavity) could be found easily. For 20 800 Mc/sec and 1°K, $2\mu_0H/kT=1$. The spectrometer is provided with a Pound i.f. stabilization system.[28,29] The klystron stabilizer is generally not used during the saturation of the various transitions of the radioactive element; instead the klystron reflector is modulated with a low-amplitude sine wave and the frequency is continuously monitored by observing the rectified output of the klystron on an oscilloscope. When high sensitivity is desired the magnetic field is modulated with the 60-cycle line voltage; a lock-in detector using a 6AR8 beam switching tube and a Varian recorder is used to record the signals.

The cryostat (Fig. 17) is made entirely of metal[30] and has a 15-in. long, 2-in. o.d. tail which fits into the magnet gap. The connecting pipe between the helium pot and the liquid air chamber is a piece of stainless steel tubing 1.125 in. i.d., 6 in. long, with a 0.004-in. wall. The helium pot holds 1.2 liters. When baffles are placed around the inserted wave guide to prevent oscillations in the helium column, one charge of helium will last 8 to 10 hours after the cryostat is pumped down to 1.25°K. A large (60 ft^3/min) Stokes pump is used to reach a temperature of 1.25°K.

A single length of copper wave guide is inserted into the cryostat. It is provided with a 13-in. long, 0.005-in. wall piece of stainless steel wave guide obtained from the Superior Tube Company for a thermal insulation section. Rectangular cavities operating in a TE_{10n} mode are used to contain the sample; the cavities are broken $3\lambda_g/4$ below the coupling iris for insertion of the sample. All of the silicon samples are cut so that they have the same cross section as the wave guide.

For the double resonance experiments a different type

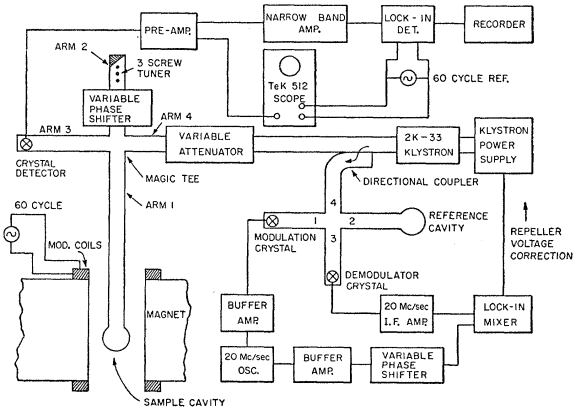

FIG. 13. Paramagnetic resonance spectrometer.

[26] M. E. Rose, Phys. Rev. **53**, 715 (1938).
[27] N. J. Hopkins, Rev. Sci. Instr. **20**, 401 (1949).
[28] R. V. Pound, Proc. Inst. Radio Engrs. **35**, 1405 (1947).
[29] Tuller, Galloway, and Zaffarano, Proc. Inst. Radio Engrs. **36**, 794 (1948).
[30] W. E. Henry and R. L. Dolecek, Rev. Sci. Instr. **21**, 496 (1950).

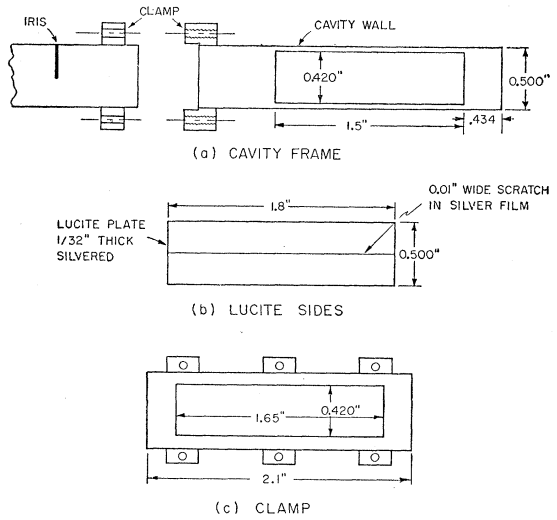

FIG. 14. Plan view of rectangular cavity with silvered Lucite sides which was used for double resonance experiments.

of cavity is used. A diagram of this cavity is shown in Figs. 14 and 15. The sides of the cavity are made of thinly silvered Lucite; the silvering thickness is such that a fluorescent room light can just barely be seen through the silvering. The scratch down the center is essential to break the path of shielding currents. This cavity is insulated with Scotch masking tape and a coil consisting of 12 turns of No. 17 Formex wire wound around it. Several layers of Scotch masking tape are placed on one side of the wave guide reaching up its entire length. A piece of $\frac{1}{16}$-in. diameter copper wire with a 13-in. long, $\frac{1}{16}$-in. diameter stainless steel tube for thermal insulation is fastened in the center of the masking tape. This wire together with the wave guide forms a 50 ohm strip line, and it is used to connect to the coil at the lower end of the wave guide. The strip line is joined at the top of the cryostat to RG 8/U cable. For monitoring the radio-frequency magnetic field, 12 turns of No. 28 wire are wrapped around the radio-frequency coil in such a fashion as to be primarily sensitive to the magnetic flux. The leads are brought out through fine advance wire to a 1*N*34 crystal in series with a microammeter.

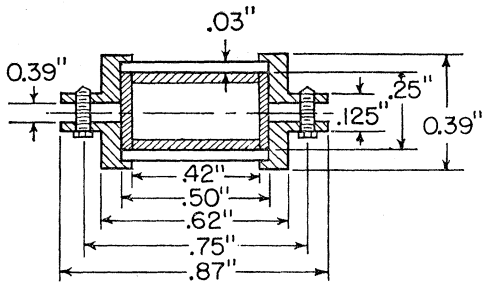

FIG. 15. Cross-sectional view of cavity used in double resonance experiments.

A Hewlett Packard 608C signal generator provided with a small tuned power amplifier is used as a source of radio-frequency power in the 10 to 70 Mc/sec range. A general Radio 1208B unit oscillator is used for higher frequencies (60→200 Mc/sec). For frequency measurement a General Radio 620A heterodyne frequency meter is used in conjunction with a General Radio 720A frequency meter.

A block diagram of the counting equipment is shown in Fig. 16. A $1\frac{1}{2}$-in. by 1-in. NaI(Tl) crystal purchased from the Harshaw Chemical Company and an RCA 6342 photomultiplier are used to detect the gamma rays. A carefully flame-polished Lucite light pipe 13 in. long and 1.5 in. o.d. joins the crystal and the magnetically shielded photomultipler. A 15% resolution is obtained for the Cs^{137} gamma-ray photopeak. The pulse amplifier is a Los Alamos 501 modified to reduce the overload problem. In order to reduce the drift of the counter, a feedback system similar to that described by De Waard[31] is used to maintain the photopeak of As^{76} at a constant voltage. This system makes it possible to

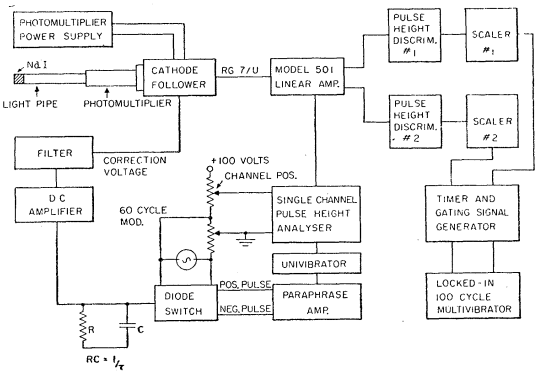

FIG. 16. Block diagram of counting equipment.

maintain the counting rate to within $(2N)^{\frac{1}{2}}$ independent of the magnetic field and over considerable lengths of time. The 100-cycle multivibrator signal derived from the General Radio-Frequency Standard in the laboratory is used to gate the counters on and off. In the usual cycle of operation the counters are on for 90 seconds and then off for 10 seconds while they are being read.

In its normal position (*A* of Fig. 17) the counter views the number of gamma-rays emitted in a direction perpendicular to the direction of the static magnetic field. For the analysis of the beta decay, it is desirable to measure the change in counting rate for both the σ and π positions. In the course of the experiment, it was discovered that when the nuclei were oriented, the orientation persisted for a long time (2–3 hours). Consequently, the following scheme was adapted for observing the counting rate changes in the π position. The counter was placed in position *B* of Fig. 17. While the counter was in the magnet, it was in the σ position.

[31] H. De Waard, Nucleonics **13**, No. 7, 36 (1955).

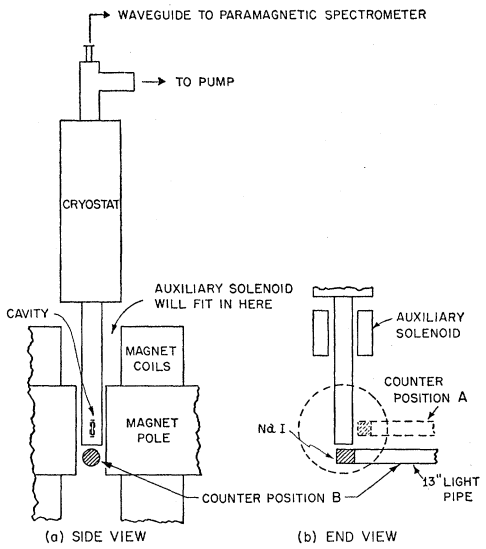

FIG. 17. Diagram showing the two positions of the counter. *A* was used for measurements in the σ position and *B* for measurements in the π position.

If the magnet was rolled away and the small solenoid lowered and turned on, the counter was in the π position.

EXPERIMENTAL PROCEDURE

The arsenic-doped silicon crystals were obtained from the Raytheon Manufacturing Company. The nominal doping was 4.5×10^{16} donors/cm^3. The doping as measured by the neutron induced actively in this crystal and in a known weight of As_2O_3 was 2.8×10^{16} donors/cm^3. The sample was cut from the slab furnished by the Raytheon Company into a block 0.420 in. by 0.170 in. and of such a length (1.140 in. in this case) that cavity resonances could be easily found when the sample was inserted into the microwave cavity. The sample was then encased in a quartz capsule and sent away to be irradiated. Early irradiations were made at Brookhaven National Laboratory; subsequent ones were made in the Materials Testing Reactor at Arco, Idaho. The irradiations at Brookhaven were made for a 3-day period in a flux of 3×10^{12} thermal neutrons/cm^2 sec. The irradiations made in Idaho were for a 24-hour period in a flux of 10^{14} thermal neutrons/cm^2 sec. Upon return from being irradiated, the sample was etched with CP-4 reagent to remove Na^{24} contamination from the surface. It was found that sodium from hand contact produced as much activity upon irradiation as the As^{76}. The sample was placed in a quartz tube. This tube was evacuated and placed in an electric furnace where the sample was annealed 4 to 6 hours at 1100–1200°C to heal radiation damage. No permanent changes in the crystals were observed; each crystal was bombarded several times. The sample was then placed in the microwave cavity and immersed in helium. Once a suitable cavity mode was found and the gamma-ray spectrum had been determined, the cryostat was pumped down to 1.25°K. The counting-rate integral discriminator was then set so that it was in the valley below the 550-kev photopeak. To establish a known equilibrium starting state, the magnet was always rolled away so that the As^{76} could relax in zero magnetic field. After 10 minutes at zero field, the magnet was rolled back and experiments begun. Counts were taken for 90 sec periods. Three such readings were totaled and the result immediately corrected for decay.

RESULTS OF THE EXPERIMENT

A. Measurement of Hyperfine Splitting of As^{76}

The As^{76} was first oriented successfully by saturation of the $(\frac{1}{2},m_I)\rightarrow(-\frac{1}{2},m_I+1)$ forbidden transitions. For these experiments the microwave cavity was turned so that there was a component of the microwave magnetic field parallel to the static magnetic field. The static field was then moved slowly over the region where the resonances of the stable As^{75} occurred. Plots of counting rate *versus* magnetic field for movement both from high to low field and from low to high field are shown in Fig. 18. These curves show the presence of two transitions which are approximately symmetrically located about the center of the As^{75} hyperfine structure. They also indicate that the nuclear relaxation time is greater than 30 minutes; the alignment does not decay between

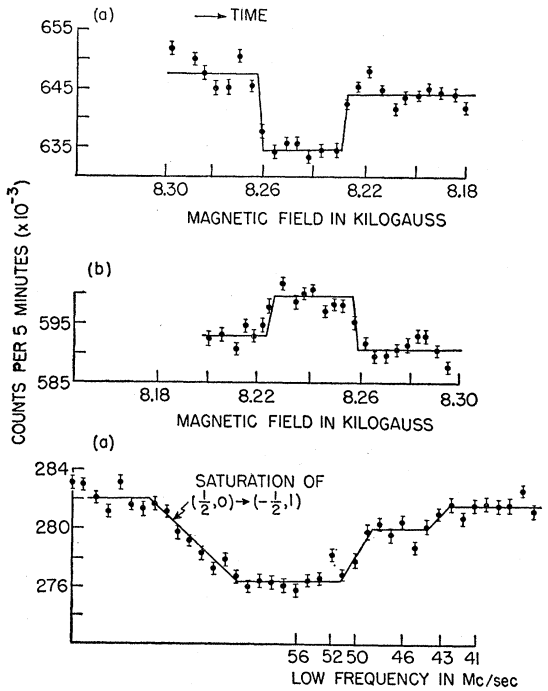

FIG. 18. (a) Plot of counting rate *versus* magnetic field for saturation of the forbidden transitions. Movement is from high to low field. (b) Same as (a), only with movement from low to high field. (c) Formation of orientation by saturation of $(\frac{1}{2},0)\rightarrow(-\frac{1}{2},1)$ transition and subsequent destruction of orientation by the low frequency.

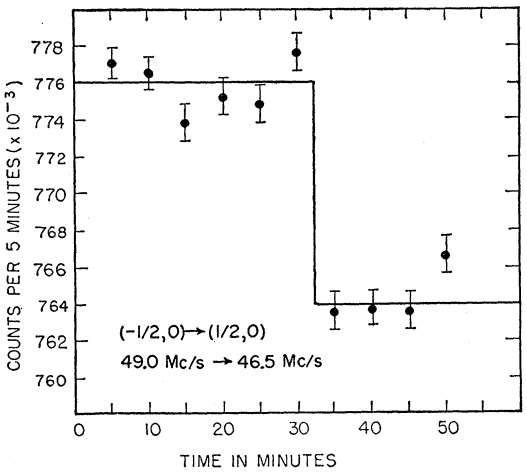

FIG. 19. Double fast-passage experiment to determine sign of the counting rate change in the σ position for an increase of the population of the $m_I=0$ states. The levels $(\frac{1}{2},0)$ and $(-\frac{1}{2},0)$ were inverted and then the low frequency swept from 49 to 46.5 Mc/sec.

the two transitions but remains and is just cancelled by the second transition.

In order to determine whether these two transitions were the pair $(\frac{1}{2},0)\rightarrow(-\frac{1}{2},1)$ and $(\frac{1}{2},-1)\rightarrow(-\frac{1}{2},0)$ or the pair $(\frac{1}{2},-2)\rightarrow(-\frac{1}{2},-1)$ and $(\frac{1}{2},1)\rightarrow(-\frac{1}{2},2)$, a double resonance experiment was performed. The observed separation of the lines is 34 gauss; consequently, if the transitions are the pair $(\frac{1}{2},0)\rightarrow(-\frac{1}{2},1)$ and $(\frac{1}{2},-1)\rightarrow(-\frac{1}{2},0)$ the nuclear transitions $(m_J,m_I)\rightarrow(m_J, m_I+1)$ would occur about 46 Mc/sec. If the transitions are the $(\frac{1}{2},-2)\rightarrow(-\frac{1}{2},-1)$ and $(\frac{1}{2},1)\rightarrow(-\frac{1}{2},2)$ the nuclear transitions would occur at about 16 Mc/sec. To determine which hypothesis was correct, alignment was produced by saturation of the high-field transition of Fig. 18(a). The low-frequency oscillator was then swept through the regions of 16 and 46 Mc/sec. The results of this experiment are shown in Fig. 18. The alignment was partially destroyed at 44 and 49 Mc/sec. No effect was observed at 16 Mc/sec. Consequently, the two transitions are $(\frac{1}{2},0)\rightarrow(-\frac{1}{2},1)$ and $(\frac{1}{2},-1)\rightarrow(-\frac{1}{2},0)$.

To determine the sign of the nuclear magnetic moment a double resonance experiment was performed to find the sign of the effect produced by increasing the population of the $m_I=0$ levels. The level pair $(\frac{1}{2},0)\rightarrow(-\frac{1}{2},0)$ were inverted and then the low-frequency oscillator swept from 49 to 46.5 Mc/sec. This second operation would correspond to the inversion of the levels $(-\frac{1}{2},0)$ and $(-\frac{1}{2},1)$ if the moment were negative and the inversion of the levels $(-\frac{1}{2},0)$ and $(-\frac{1}{2},-1)$ if the moment were positive. In either case the population of the $m=0$ level would be increased. The result of this experiment is shown in Fig. 19. The counting rate in the σ position decreases for an increase in the population of the $m_I=0$ states. Comparison of this result with Fig. 10 and Fig. 18 shows that the nuclear magnetic moment must be negative. The center of gravity of the forbidden lines was also shifted from the center of

TABLE VI. Measured values of the nuclear transition frequencies. These values were determined from the curves shown in Fig. 20. The direction signifies whether the measurement was made with increasing or decreasing frequency. The static magnetic field was 8350 gauss.

Direction	Transition	Measured frequency in Mc/sec	Calculated $A/2$ in Mc/sec
Up	$(-\frac{1}{2},1)\rightarrow(-\frac{1}{2},0)$	49.719	46.839
Down	$(-\frac{1}{2},1)\rightarrow(-\frac{1}{2},0)$	49.752	46.872
Up	$(-\frac{1}{2},0)\rightarrow(-\frac{1}{2},-1)$	49.518	46.826
Down	$(-\frac{1}{2},0)\rightarrow(-\frac{1}{2},-1)$	49.629	46.924
		Mean =	46.865

gravity of the electron resonance lines of the stable isotope by $+2.0\pm1$ gauss in agreement with the effect expected for a negative nuclear moment.

To obtain a more precise value of the hyperfine splitting, a more careful double resonance experiment was performed. First the transition $(\frac{1}{2},0)\rightarrow(-\frac{1}{2},1)$ was saturated. The low-frequency oscillator was then swept at 10 (kc/sec)/min over the region of the 49.5-Mc/sec nuclear transitions. It was swept first from high to low frequency and then from low to high frequency. The orientation was destroyed by saturation of the $(-\frac{1}{2},0)\rightarrow(-\frac{1}{2},1)$ and the $(-\frac{1}{2},0)\rightarrow(-\frac{1}{2},-1)$ nuclear transitions. Two such curves taken at 8350 gauss are shown in Fig. 20. In Table VI are summarized the values of the hyperfine splitting obtained from this set of data. The transition frequency is taken as the frequency at which the orientation has been reduced by one-half of the full decrease for that particular transition. The disagreement between the two values for the same transition but with a different direction of approach indicates that the orientation is more than half-gone before the center of the line is reached. From the shapes of the curves and the separation of the two frequencies for opposite direction of approach, it is concluded that the nuclear line width is approximately 100 kc/sec. From this measurement, the value

$$A^{76}=-93.730\pm0.100 \text{ Mc/sec}$$

is obtained for the hyperfine splitting. In Table VII are summarized the various determinations of the hyperfine splitting. A weighted average gives the final value

$$A^{76}=-93.660\pm0.06 \text{ Mc/sec}. \quad (36)$$

To show that the spin was 2 a more careful attempt was made to detect the $(\frac{1}{2},1)\rightarrow(-\frac{1}{2},2)$ transition. A search with better counter stability and a more active source showed that there was a small change in counting

TABLE VII. Hyperfine splittings of radioactive As^{76} determined in various runs.

A (Mc/sec)	Prob. error
93.510	±0.200
93.730	±0.100
93.620	±0.100

rate at the proper magnetic field. Also, when this transition was saturated and the counter changed to position B as will be described in the section on the beta-decay, a 3% change in counting rate was observed. This is shown in Fig. 23. No evidence for higher spin was obtained.[32]

B. Measurement of the Hyperfine Splitting of As^{75}

In order to determine the gyromagnetic ratio of the unstable As^{76} from the measurement of the hyperfine splitting, it is necessary to make a precise determination of the hyperfine splitting of the stable As^{75}. This was done by the electron-spin double resonance method.[33] The energy levels of the As^{75} donor in a strong magnetic field are depicted in Fig. 21. The magnetic field and the microwave power level were adjusted so that the transition $(-\frac{1}{2},-\frac{3}{2})\rightarrow(\frac{1}{2},-\frac{3}{2})$ was being partially saturated. The lock-in-detector and recorder previously mentioned were used to monitor the microwave signal. A second radio-frequency oscillator of about 106 Mc/sec was then swept over the region of the nuclear transitions $(-\frac{1}{2},-\frac{3}{2})\rightarrow(-\frac{1}{2},-\frac{1}{2})$ and $(\frac{1}{2},-\frac{1}{2})\rightarrow(\frac{1}{2},-\frac{3}{2})$. This enhances the electron resonance and the enhancement can be seen on the recorder. This process was repeated numerous times with various power levels and with opposite directions of approach. Two recorder tracings for the $(-\frac{1}{2},-\frac{3}{2})\rightarrow(-\frac{1}{2},-\frac{1}{2})$ transition are shown in Fig. 22.

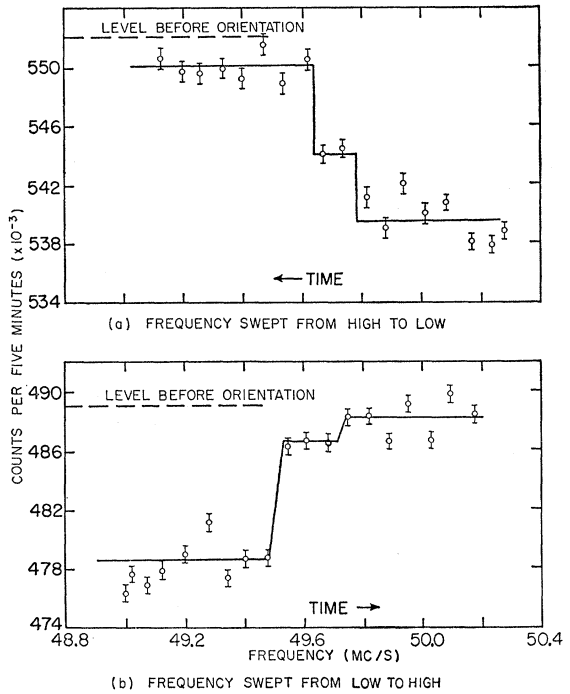

FIG. 20. Plots of counting rate *versus* frequency for the precise determination of the hyperfine splitting. Orientation was produced by saturation of the $(\frac{1}{2},0)\rightarrow(-\frac{1}{2},1)$ transition. The magnetic field was 8350 gauss and the oscillator was swept at 10 (kc/sec)/min.

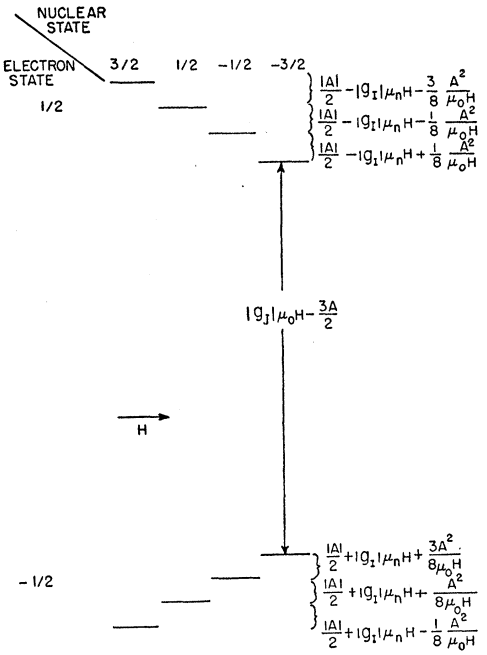

FIG. 21. Energy levels for As^{75} donor in a large magnetic field ($\mu_0 H \gg A$). The arrow with an H indicates the order in which the lines are displayed as a function of magnetic field for a fixed oscillator frequency.

As has been pointed out by Feher,[33] the line shape observed is not the line shape for the nuclear transition; it is just a measure of the excess spins in the top level of the electron transition. The peak of the curve occurs at the point where the rate of addition (or subtraction) of spins just equals the rate of saturation. The line width must be at least as great as the rising part of the observed signal. The amount by which it is greater than this is given by the shift of the half-amplitude of the rising portion of the line for the two directions of frequency sweep. Such an analysis indicates that the line width is 80 kc/sec. From a number of such observations, it is concluded that for a field of 8520 gauss, the frequency of the $(-\frac{1}{2},-\frac{3}{2})\rightarrow(-\frac{1}{2},-\frac{1}{2})$ transition is

$$106.65\pm0.02 \text{ Mc/sec.}$$

From the second-order expression for this transition,[34]

$$h\nu_{(-\frac{1}{2},-\frac{3}{2})\rightarrow(-\frac{1}{2},-\frac{1}{2})}=\tfrac{1}{2}A+g_I\mu_n H+(3A^2/8\mu_0 H),$$

and the known gyromagnetic ratio of As^{75},

$$g_I{}^{75}=0.95931,$$

[32] The measurement of the spin has been confirmed by a completely unambiguous atomic beam method. Christensen, Bennewitz, Hamilton, Reynolds, and Stroke, Phys. Rev. **107**, 633 (1957).

[33] G. Feher, Phys. Rev. **103**, 834 (1956).

[34] N. F. Ramsey, *Nuclear Moments* (John Wiley and Sons, Inc., New York, 1953), Chap. 3, p. 51.

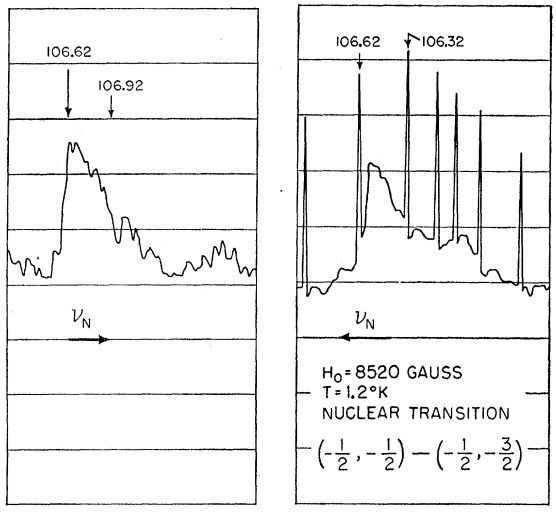

FIG. 22. Recorder tracings of electron spin double resonance signals for As^{75}.

we obtain for the hyperfine splitting

$$A^{75}=+198.42\pm0.04 \text{ Mc/sec.} \quad (37)$$

The Fermi-Segrè formula[35] can now be used to calculate the gyromagnetic ratio of As^{76}:

$$g^{76}=-[0.4514\pm0.0004][1+\Delta_{75,76}]. \quad (38)$$

$\Delta_{75,76}$ is the error due to the hyperfine anomaly. It should be less than 0.5% in arsenic.

C. Determination of the Relative Contributions of the Various Angular Momenta to the 2.41-Mev Beta Decay

For an unambiguous determination of the beta-decay components, it is necessary to measure the changes in counting rate in both the σ and π positions. For these experiments counter position B of Fig. 17 was used. In Fig. 23 are shown the plots of counting rate *versus* time for formation of orientation in the σ position by the saturation of the $(-\frac{1}{2},-1)\rightarrow(\frac{1}{2},-2)$ transition and the subsequent destruction of the orientation in the π position. These data were taken as follows. With the counter in position B, the forbidden transition was saturated for 20 to 30 minutes and the change in counting rate observed. The magnet was then pulled away so that the sample was in the 3000-gauss fringing field and the solenoid lowered around the sample. The solenoid was turned on and the main magnet turned off. This left the sample in such a position that the counter viewed the number of gamma-rays emitted along the direction of the magnetic field. After a new reference level for the counting rate had been established, the solenoid was turned off and the change in counting rate observed. Tests indicated that when the direction of the field was not changed, the fractional change in counting rate observed in this fashion was the same as that observed during formation. Consequently, it was assumed that when the direction of the magnetic field was changed, the full effect corresponding to the π position would be observed. On each run, tests were made to make sure that turning the solenoid on and off did not affect the counter. This process was repeated several times for both the $(-\frac{1}{2},1)\rightarrow(\frac{1}{2},0)$ and the $(-\frac{1}{2},2)\rightarrow(\frac{1}{2},1)$ transitions. The results together with the calculated ratios $S(\sigma)/S(\pi)$ are shown in Table VIII. The agreement between the various values of the ratios for the $(-\frac{1}{2},1)\rightarrow(\frac{1}{2},0)$ transition seems to indicate that the main variation in the magnitude of the changes observed is due to a variable alignment efficiency.

[35] E. Fermi and E. Segrè, Z. Physik **82**, 729 (1933).

TABLE VIII. The changes in counting rate observed in the σ and π positions for saturation of the various forbidden transitions. The counter was in position B of Fig. 18. The symbol r denotes the ratio $S(\sigma)/S(\pi)$.

Transition	$S(\pi)$	$S(\sigma)$	r
$(-\frac{1}{2},2)\rightarrow(\frac{1}{2},1)$	+0.037	−0.012	−0.32
$(-\frac{1}{2},2)\rightarrow(\frac{1}{2},1)$	+0.025	−0.000	−0.00
$(-\frac{1}{2},2)\rightarrow(\frac{1}{2},1)$	+0.030	−0.002	−0.07
$(-\frac{1}{2},-1)\rightarrow(\frac{1}{2},-2)$	−0.030	+0.004	−0.13
		Mean $r_O=-0.13$	
$(-\frac{1}{2},1)\rightarrow(\frac{1}{2},0)$	−0.026	−0.028	1.1
$(-\frac{1}{2},1)\rightarrow(\frac{1}{2},0)$	−0.023	−0.023	1.0
$(-\frac{1}{2},1)\rightarrow(\frac{1}{2},0)$	−0.020	−0.020	1.0
		Mean $r_I=1.03$	

In order to analyze these data to determine the mixture of angular momenta carried off by β_2, it is necessary to correct for the finite solid angle subtended by the detector and the presence of the other gamma rays. Some measurements were made of the signals obtained in the σ position for γ_3. They were the same as those observed for γ_1; consequently, it will be assumed that β_2 and β_3 carry off the same mixture of angular momenta. There are four sources of counting rate which contribute to the observed signals. They are

(1) γ_1 from β_2, (2) γ_3 from β_3,
(3) γ_1 from γ_2, (4) γ_2 from β_3.

For the analysis it will be assumed that the other gamma rays can be ignored and that the efficiency for detection of γ_1, γ_2, and γ_3 is the same. For γ_1 from β_2, the angular distribution is

$$[W(\theta)]_1=(8/7)[1-(10/7)B_2f_2P_2(\cos\theta) -(40/3)B_4f_4P_4(\cos\theta)], \quad (39)$$

where B_2 and B_4 are the factors of Eq. (21) which take into consideration the beta decay. For γ_3 from β_3, the angular distribution is

$$[W(\theta)]_2=(2/7)[1-(10/7)B_2f_2P_2(\cos\theta) -(40/3)B_4f_4P_4(\cos\theta)]. \quad (40)$$

The angular distribution for γ_1 from γ_2 can be calculated by using Eqs. (7), (8), and (9) to calculate the f_2 and f_4

parameters after γ_2 is emitted from those before it was emitted as was done for the β ray. In this case, if a_1 and a_2 represent the reduced matrix elements for the magnetic dipole and the electric quadrupole components, respectively, then

$$[W(\theta)]_3=\frac{2}{7}\left[1-\frac{10}{7}\left(\frac{a_1^2}{2}-\frac{3a_2^2}{14}\right)f_2B_2P_2 - \frac{40}{3}\left(-\frac{2a_1^2}{3}+\frac{2a_2^2}{7}\right)f_4B_4P_4\right]. \quad (41)$$

For γ_2 in Se^{76}, $a_2/a_1=-7.2\pm1.5$. Consequently Eq. (41) becomes

$$[W(\theta)]_3=(2/7)[1+(10/7)(0.2008)f_2B_2P_2 - (40/3)(0.2678)f_4B_4P_4]. \quad (42)$$

The angular distribution for γ_2 from β_3 can be calculated from the general formula[36] for the angular distribution of a mixed magnetic dipole and electric quadrupole transition. For a $j_f=j_i$ transition, the angular distribution is

$$W(\theta)=2\left\{1+\frac{1}{14}\left[-21a_1^2 +126\left(\frac{5}{(2j_i+3)(2j_i-1)}\right)^{\frac{1}{2}}a_1a_2 +15\frac{(2j_i+5)(2j_i-3)}{(2j_i+3)(2j_i-1)}a_2^2\right]K_2f_2P_2 - \frac{30}{(2j_i+3)(2j_i-1)}a_2^2K_2f_4P_4\right\}, \quad (43)$$

where j_i is the spin of the gamma emitting state and

$$K_2=j_i/(j_i+1); \quad K_4=j_i^3/(j_i+1). \quad (44)$$

Equation (44) gives for the angular distribution of γ_2 from β_2,

$$W(\theta)=(2/7)[1-(10/7)(0.0823)f_2B_2P_2 - (40/3)(0.2804)B_4f_4P_4]. \quad (45)$$

The total angular distribution can now be calculated by adding Eqs. (39), (40), (42), and (45). It is

$$W(\theta)_T=2[1-(10/7)(0.7312)f_2B_2P_2 - (40/3)(0.7926)f_4B_4P_4]. \quad (46)$$

For the equivalent reduction of f_2 and f_4 due to the finite solid angle subtended by the detector, Rose[37] gives the formula

$$f_k'=f_k\frac{P_{k-1}(x_0)-x_0P_k(x_0)}{(k+1)(x_0)}, \quad (47)$$

where $x_0=\cos\theta$ and θ is the half-angle of the cone subtended by the detector at the source. For position B of Fig. 17, $\theta=10°$. Consequently

$$f_2'=0.98f_2, \quad f_4'=0.93f_4,$$

and the observed angular distribution would be

$$W(\theta)_T=2[1-(10/7)(0.714)f_2B_2P_2 - (40/3)(0.734)f_4B_4P_4]. \quad (48)$$

Thus, for this experiment, if the observed signals are divided by 0.72, all the corrections for the various gamma rays and the finite detector solid angle will have been made. Henceforth, when speaking of the observed signals, it will be assumed that this correction has been made.

These corrected data can be analyzed in two ways to determine the restrictions on α_1 and α_2. The first method makes use of the ratios $S(\sigma)/S(\pi)$; the second uses only the effects observed in the σ position. If the ratio $r_I=1.0$ determined in Table VIII is inserted in Eq. (33), the value

$$r_O=-0.26$$

is obtained. This is not completely inconsistent with the experimental value

$$r_O=-0.13,$$

but it is disturbing. If the two experimental values for r_I and r_O are inserted into Eqs. (31) and (32), the following relationships are obtained:

$$r_O: \quad \alpha_1+0.034\alpha_2=0.32, \quad (49)$$

$$r_I: \quad \alpha_1+0.23\ \alpha_2=0.46. \quad (50)$$

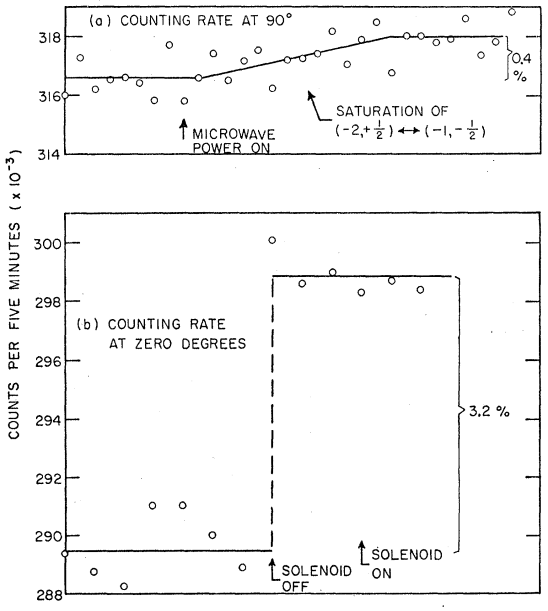

FIG. 23. (a) Plot of counting rate *versus* time for saturation of $(-\frac{1}{2},-1)\rightarrow(\frac{1}{2},-2)$ transition. Counter position B was used. (b) Plot of counting rate *versus* time for destruction of orientation in π position.

[36] Hartogh, Tolhoek, and de Groot, Physica **20**, 1310 (1954).
[37] M. E. Rose, Phys. Rev. **91**, 610 (1953).

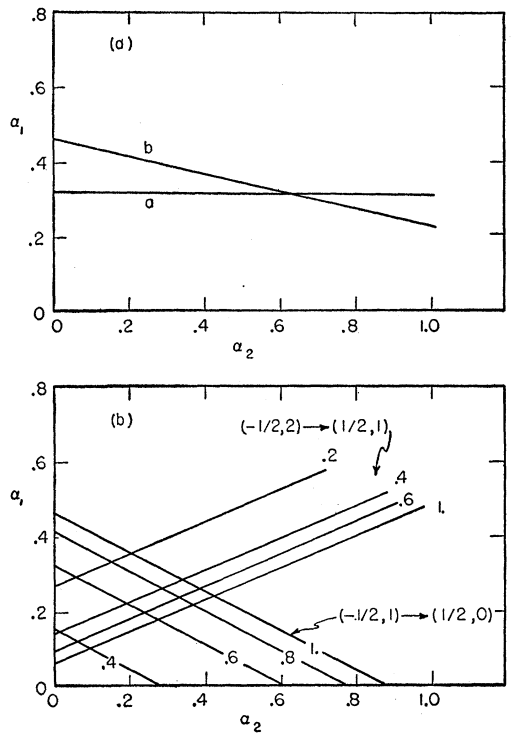

FIG. 24. (a) Possible relationship between β-decay components obtained from the two ratios r_I and r_O and the limitation on the efficiency. Line a is for outside lines and line b is for inside lines. (b) Possible relationship between beta-decay components obtained from observation of the lines in the σ position only. The small numbers beside the lines are the assumed average efficiencies.

These two lines are shown as a and b, respectively, in Fig. 24(a). Further restrictions on α_1 and α_2 can be imposed by considering the limited range of values for the efficiency. If Eqs. (29) and (30) are solved for α_2, the expression

$$\alpha_2=\frac{7}{20}\left[2-\frac{18S_I(\pi)-44S_I(\sigma)}{\eta\tanh(\mu_0H/kT)}\right] \tag{51}$$

is obtained. When the corrected experimental average values are inserted into this equation, it becomes

$$\alpha_2=\frac{7}{20}\left(2-\frac{2.08}{\eta}\right). \tag{52}$$

Since $0\leq\eta\leq1$, and $\alpha_2\geq0$, Eq. (52) says that the efficiency must be nearly 100% and α_2 must be small. Thus these data give the values

$$\alpha_0=0.6,\quad \alpha_1=0.4,\quad \alpha_2=0. \tag{53}$$

This combination predicts that for the $(-\frac{1}{2},2)\rightarrow(\frac{1}{2},1)$ transition, the signal in the σ position corrected for the other gamma rays and the solid angle attenuation would be

$$S(\sigma)=-0.0154.$$

Experimentally the average observed value was -0.0045. Thus this combination implies a low orientation efficiency for the $(-\frac{1}{2},2)\rightarrow(\frac{1}{2},1)$ transition.

The second method of analysis employs only the two observations made in the σ position. If the corrected average experimental values for the two transitions at this angle are inserted into Eqs. (29) and (30), the following relationships are obtained. For the $(-\frac{1}{2},2)\rightarrow(-\frac{1}{2},1)$ transition,

$$\alpha_1-0.43\alpha_2=0.052/\eta. \tag{54}$$

For the $(-\frac{1}{2},1)\rightarrow(\frac{1}{2},0)$ transition,

$$\alpha_1+0.524\alpha_2=0.667-0.208/\eta. \tag{55}$$

For various values of the efficiency, these two sets of lines have been plotted in Fig. 24(b). Since the average values have been used, the efficiency will not be expected to be 100%. If it is assumed that the largest signals observed represent 100% efficiency, then the average efficiency can be estimated to be 80%. A comparison of Fig. 24(a) and Fig. 24(b) shows that either a very low orientation efficiency for the $(-\frac{1}{2},2)\rightarrow(\frac{1}{2},1)$ transition must be assumed or that the observed ratios are wrong. Both alternatives seem disagreeable. The uncertainty can only be resolved by an experiment in which both the σ and π counting rates are observed simultaneously. The best assumption seems to be that the ratios are incorrect for some unknown reason. If this is assumed, the following restriction can be placed on the β-decay components:

$$\begin{aligned}&0.1\leq\alpha_1\leq0.4,\\&0.1\leq\alpha_2\leq0.4,\\&0.2\leq\alpha_0\leq0.6.\end{aligned} \tag{56}$$

D. Unsuccessful Orientation Experiments

Two separate series of attempts were made to observe the alignment produced by the Abragam method. In the first series of experiments a pair of small Helmholtz coils were placed around the tail of the cryostat so that an auxiliary magnetic field variable from 0 to 100 gauss could be produced either in the direction of or perpendicular to the axis of the counter. The silicon sample was placed in a field of 11 000 gauss for a period of 30 minutes or more. The auxiliary coils were then turned on and the magnet rolled away. The auxiliary magnetic field was switched so that the counter viewed the σ and π positions in rapid succession. The counts were fed to two separate scalers. In effect the whole system acted like a lock-in-detector; in this manner the counter drift was eliminated. For variation of the auxiliary field between 10 and 80 gauss, no difference of counting rate $>0.1\%$ was observed. Tests made without the switching revealed no asymmetries $>0.5\%$. The expected difference for the observed β-ray mixture is about 5.0%.

In the second set of experiments the auxiliary solenoid

of counter position B was used. In this case the sample was placed in a magnetic field of 11 000 gauss for 30 minutes or more. The magnet was pulled away partially so that the sample was in the 3000-gauss fringing field and the solenoid lowered. The solenoid was turned on and the main magnet turned off. The solenoid field was varied from 500 to 1500 gauss in different runs. The field of the solenoid was then decreased to various values less than 100 gauss for various periods of time. It was then returned to 1500 gauss. The counting rate was monitored to establish a reference level and subsequently the solenoid was turned off to destroy any orientation. No effects greater than 1% were observed. The expected change is only 2%.

In the course of the experiment many attempts were made to observe the Overhauser orientation. When the As^{76} had been successfully aligned, the relaxation time for the orientation was measured and found to be 200 minutes[25]; consequently, it would take a long time for the Overhauser orientation to develop even if this relaxation is due to the proper mechanism. All the lines have been saturated for periods up to one hour with no effects $>3\%$ observed. The effect expected for the total Overhauser effect is 17%. Also the $(-\frac{1}{2},0)\rightarrow(\frac{1}{2},0)$ transition was saturated for 150 minutes. Here the final change should only be 1.5%. No changes greater than 1% were observed.

CONCLUSIONS

The nuclear magnetic moment of As^{76} has been found to be

$$\mu^{76}=-0.9028\pm0.005\ \mu_n.$$

The precision is limited by the hyperfine anomaly. The usual shell-model configuration assigned to As^{76} is $f_{5/2}-g_{9/2}$. If the simple j-j coupling model is used to calculate the magnetic moment from the empirical g values for the $f_{5/2}$ proton and the $g_{9/2}$ neutron, the value

$$\mu_{\text{theo}}=-1.83\ \mu_n$$

is obtained. This value is wrong by a factor of 2.

The present systematic uncertainties of the data prevent a firm estimate of the relative contributions of the various angular momenta to the beta decay. It is clear, however, that when the experiment is performed with the suggested modification, it should be possible to restrict them quite precisely. When the experiment is redone, it should also be possible to use this data in conjunction with data from the spectrum shape, the angular correlation, and the correlation experiments made possible by the nonconservation of parity to determine all 6 of the nuclear matrix elements which enter into the expressions for α_0, α_1, and α_2 in case the fundamental beta interaction is a mixture of vector and axial-vector.

ACKNOWLEDGMENTS

We are especially indebted to Professor R. V. Pound for expressing interest in this experiment and for continued advice throughout its execution. We would also like to thank the Raytheon Company for supplying the silicon crystal used in the experiment.